

# Explainable Fingerprint ROI Segmentation Using Monte Carlo Dropout

Indu Joshi\*

indu.joshi@cse.iitd.ac.in

Riya Kothari\*\*†

rskothar@usc.edu

Ayush Utkarsh\*\*‡

ayushutkarsh@gmail.com

Vinod K Kurmi§

vinodkk@iitk.ac.in

Antitza Dantcheva¶

antitza.dantcheva@inria.fr

Sumantra Dutta Roy\*

sumantra@ee.iitd.ac.in

Prem Kumar Kalra\*

pkalra@cse.iitd.ac.in

## Abstract

A fingerprint Region of Interest (ROI) segmentation module is one of the most crucial components in the fingerprint pre-processing pipeline. It separates the foreground fingerprint and background region due to which feature extraction and matching is restricted to ROI instead of entire fingerprint image. However, state-of-the-art segmentation algorithms act like a black box and do not indicate model confidence. In this direction, we propose an explainable fingerprint ROI segmentation model which indicates the pixels on which the model is uncertain. Towards this, we benchmark four state-of-the-art models for semantic segmentation on fingerprint ROI segmentation. Furthermore, we demonstrate the effectiveness of model uncertainty as an attention mechanism to improve the segmentation performance of the best performing model. Experiments on publicly available Fingerprint Verification Challenge (FVC) databases showcase the effectiveness of the proposed model.

## 1. Introduction

Fingerprint matching systems are one of the most robust biometrics-based authentication systems. Owing to the low cost of fingerprint sensors, it is used for a plethora of applications ranging from access control, online payments to getting subsidies through government welfare schemes. Although fingerprint matching systems are generally quite robust, however, it is observed that fingerprint matching performance is adversely affected due to presence of background noise.

\*Indian Institute of Technology Delhi, India

†University of Southern California, USA

\*\*Equal contributions from both authors.

‡Independent Researcher, India

§Indian Institute of Technology Kanpur, India

¶Inria Sophia Antipolis, France

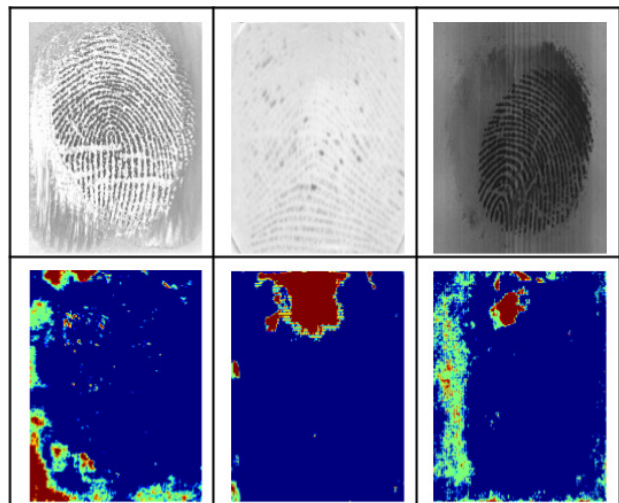


Figure 1. **Visualization of model uncertainty** in Fingerprint ROI segmentation. First row showcases samples from FVC databases while second row illustrates the obtained model uncertainty. The visualization of uncertainty values demonstrates the fact that the model outputs higher uncertainty around noise and pixels with unclear ridge structure (blue and red color denote low and high uncertainty values respectively).

Fingerprint region of interest (ROI) segmentation is typically the first step in fingerprint pre-processing pipeline. This step is targeted to separate the foreground fingerprint and background region. Foreground fingerprint region is identified by fingerprint region with clear textured patterns containing ridges and valleys whereas the background constitutes of sensor noise or noise originating due to oil and dirt on the surface of sensor. Fingerprint ROI segmentation helps the fingerprint matching system two folds: firstly, it restricts the area for fingerprint feature extraction only in the foreground. Thus, minimises the possibility of spurious feature (minutiae) extraction around the boundary of foreground fingerprint. Furthermore, ROI segmentation elimi-

nates the chances of erroneous detection of minutiae due to sensor noise around image boundaries. Secondly, it reduces the computation time for performing matching.

Fingerprint image can be acquired from a variety of sensors employing different sensing technology such as optical, capacitive and thermal (see first row of Figure 1). Furthermore, different fingerprint scanners, even when utilizing same sensing technology introduce varying sensor noise in the fingerprint images, depending upon the vendor manufacturing the scanning device. Varying background noise originating from disparate sensors adversely affects the generalization performance of fingerprint ROI segmentation algorithm. In such cases, *uncertainty* quantification is helpful as it allows experts to assess the trustworthiness of predictions and can prevent erroneous ones.

Towards designing an explainable fingerprint ROI segmentation model, we aim to design a model which outputs an *uncertainty* score for each pixel which can help to understand whether the model is confident in its prediction or not (See second row of Figure 1). This can help to identify scenarios where human intervention can help to minimize error in model’s prediction. We also hypothesize that while learning to quantify uncertainty in prediction, model implicitly learns the relative importance of features and adjusts the model weights accordingly. As a result, training the fingerprint ROI segmentation model to incorporate the notion of explainability through model uncertainty acts like an attention mechanism and helps to improve segmentation performance.

## 2. Related Work

**Filtering in Fourier domain:** Hu *et al.* [10] propose fusion based segmentation algorithm. The first mask is obtained using adaptive thresholding on log-gabor filtered image whereas the second mask is obtained using orientation reliability information. Thai *et al.* [28] argue that the frequencies in Fourier spectrum of fingerprint images lie only in specific band. Authors propose factorized directional bandpass filtering in Fourier domain to obtain the segmentation mask.

**Morphological operations based segmentation:** Thai and Gottschlich [27] propose a three part decomposition method to separate the noise and fingerprint image. Morphological operations on the binarized fingerprint image are performed to obtain the ROI mask. Fahmy and Thabet [6] compute the range image for the input fingerprint image. The range image is then converted into binary image using adaptive thresholding. Morphological operations and contour smoothing is applied over the binary image to obtain ROI mask.

**Ridge orientation information based segmentation:** Teixeira and Leite [26] propose monotonic filtering of image extrema using multi-scale pyramidal structuring ele-

ment and orientation of each pixel is obtained using multi-scale directional operator. Segmented image is obtained using the computed directional field. Raimundo *et al.* [4] propose orientation based quality measure to identify pixels parallel and perpendicular to the flow of ridge orientation. Clustering is performed to find non-overlapping regions with distinct quality.

**Learning based segmentation algorithms:** Ferreira *et al.* [7] and Yang *et al.* [31] propose clustering of pixels to segment fingerprints. Liu *et al.* [19] proposes handcrafted intensity and texture features to classify a patch as foreground or background. Serafim *et al.* [23] and Stojanović *et al.* [25] propose classification of image patches using a convolutional neural network (CNN).

To summarize, the fingerprint ROI segmentation algorithms explained above are not end-to-end models. Rather, the models work on patch level. As a result, to overcome the block-effect observed in these models, these require post-processing to output the segmentation mask.

**Uncertainty Estimation:** It has been observed that the deep learning models are overconfident even for the wrong prediction [20]. Thus, obtaining uncertainty in the prediction of deep learning models may help to overcome this issue. Bayesian neural network (BNN) is well suited to obtain the estimation of uncertainty. However, optimization of BNN is intractable. To overcome this, later Gal *et al.* [8] show that dropout based model can work as the approximation of BNN. Blundell *et al.* [1] present an efficient method to obtain uncertainty in weights by backpropagation in BNN. Data and model uncertainty are modeled in [15]. Prior network [21] uses the Dirichlet distribution matching for detection the out of distribution samples. Ensemble models are also capable to capture the uncertainty estimation [18]. Bayesian uncertainty estimation in deep learning are discussed in [14, 16, 29].

All of the fingerprint ROI segmentation algorithms proposed so far in the literature act like a black-box and do not indicate which pixels are highly likely to be erroneous. Motivated by the success of uncertainty in various applications [15, 3, 17], we propose an explainable fingerprint ROI segmentation model which not only predicts ROI mask but also predicts an uncertainty mask which explains the confidence of prediction by the proposed model.

### 2.1. Research Contributions

Most of the models proposed in the fingerprint ROI segmentation literature are not end-to-end, and require post-processing. Therefore, true uncertainty cannot be evaluated on them using Monte Carlo Dropout (as the per-pixel label might change due to post-processing). Therefore, to introduce uncertainty based explainability in a fingerprint ROI segmentation model, the baseline model must be an end-to-end model. Towards this, we benchmark the performance

of four state-of-the-art semantic segmentation models on fingerprint ROI segmentation. Having found the best performing segmentation model among the evaluated models, we modify the network architecture such that model uncertainty in segmentation is obtained. To the best of our knowledge, this is the first work to introduce uncertainty guided explainability in the fingerprints domain.

### 3. Benchmarked Algorithms

We benchmark the performance of the following state-of-the-art segmentation models on Fingerprint ROI segmentation.

- **Conditional Generative Adversarial Network (CGan):** CGan [12] employs adversarially trained generator and discriminator sub-networks. Given the input image, generator is trained to generate an output image corresponding to the input image whereas the discriminator is trained to classify whether the generated image is real or fake. The adversarial training ensures that the output image generated by the generator network corresponds to the input image while being realistic looking. CGan has previously been successfully exploited for fingerprint enhancement by Joshi *et al.* [13].
- **Unet:** Unet [22] is a convolutional neural network which has an encoder-decoder architecture. However, a Unet architecture has skip connections from encoding layer to decoding layers. The skip connections employed in the Unet architecture provide contextual information from neighbouring pixels. This helps the model to preserve edge-level details. The compactness of Unet makes it a widely used architecture for applications with small training dataset.
- **CCNet:** CCNet [11] is a fully convolution neural network that employs criss-cross attention module. The attention module helps CCNet to aggregate contextual information in horizontal and vertical direction without excessively increasing the computational overhead. Furthermore, it adopts a recurrent strategy to obtain global information from the image. This helps the model to learn contextual information and obtain good segmentation performance.
- **Recurrent Unet (RUnet):** RUnet [30] is specifically designed to take care of applications in which the amount of training dataset is small. This makes it suitable for fingerprint ROI segmentation task since the size of training dataset is fairly small. Towards ensuring compact architecture, RUnet adds recurrent unit into the baseline Unet architecture which iteratively refines both the internal state of the network and the seg-

mentation mask. This boosts the performance of standard Unet architecture without increasing too many parameters which helps to avoid overfitting.

## 4. Model Uncertainty

The deep learning based models benchmarked in Section 3 are deterministic models and are not designed to capture model uncertainty. Although these do predict probabilities at the last layer, however authors in [9] show that a model can be uncertain even if it makes a prediction with a high probability. Therefore, the predictive probability cannot be taken as a metric to quantify the confidence of a model. To calculate uncertainty from a deterministic deep model, it is required to convert it into a probabilistic model so that statistical analysis of model's prediction can be performed. We next discuss about probabilistic models and how to convert a deep model into a Bayesian deep model in order to obtain model uncertainty.

### 4.1. Bayesian Neural Networks

Let us denote training set of input images as  $X = \{x_1, x_2, \dots, x_N\}$  and its associated output ROI segmented mask as  $Y = \{y_1, y_2, \dots, y_N\}$ . For a given model  $y = f^w(x)$ , Bayesian neural networks infer the distribution over model parameters  $w$  which could have generated the observed output  $Y$ . Let the probability distribution of output given the input is denoted as  $p(y|x, w)$ . Through training, Bayesian neural network learns the posterior distribution  $p(w|X, Y)$  and determines the most likely model parameters given the set  $X$  and  $Y$ . For a given test input  $x_{test}$ , the output probability is computed as:

$$p(y_{test}|x_{test}, X, Y) = \int p(y_{test}|x_{test}, w)p(w|X, Y)dw$$

The posterior probability  $p(w|X, Y)$  required for the inference is intractable for a deep neural network. Variational Inference is one of the techniques to approximate the posterior  $p(w|X, Y)$ . It requires defining an approximating variational distribution  $q_\theta(w)$  where  $\theta$  denotes the variational parameters and  $q_\theta(w)$  is required to be close to the true posterior.

### 4.2. Dropout Approximate Inference

Given a deterministic neural network, Gal and Ghahramani [9] show that by re-parameterization of the approximate variational distribution  $q_\theta(w)$  as Bernoulli, it is possible to approximate variational inference from a deterministic neural network.

Through dropout [24] one samples binary variable for each each input and for every network unit in each layer. Let  $y_i$  denotes the output of layer  $i$ . Through application of

drop out

$$\begin{aligned} y_i &= r_i * y_i \\ y_i &= \text{Bernoulli}(r_i) y_i \end{aligned}$$

where  $r_i$  denotes the probability of binary variable to take value 1 in layer  $i$ . This demonstrates that Bayesian inference can be approximated from a deterministic neural network by incorporating dropout in its layers.

### 4.3. Calculating Model Uncertainty

$$\begin{aligned} p(y_{test}|x_{test}, X, Y) &= \int p(y_{test}|x_{test}, w) p(w|X, Y) dw \\ &\approx \int p(y_{test}|x_{test}, w) q_\theta(w) dw \\ &= \frac{1}{\tau} \sum_{t=1}^{\tau} p(y_{test}|x_{test}, \tilde{w}_t) \end{aligned}$$

where  $\tilde{w}_t \sim q_\theta(w)$  and  $q_\theta(w)$  is the dropout distribution. This result signifies that output of the model is obtained through *Monte Carlo integration* over  $\tau$  stochastic outputs obtained through the model. Model uncertainty as captured by predictive variance is approximated as:

$$\begin{aligned} \text{var}(y_{test}) &= \frac{1}{\tau} \sum_{t=1}^{\tau} (p(y_{test}|x_{test}, \tilde{w}_t))^T p(y_{test}|x_{test}, \tilde{w}_t) \\ &\quad - E(y_{test}^T) E(y_{test}) \end{aligned}$$

where  $E(y_{test}) = \frac{1}{\tau} \sum_{t=1}^{\tau} (p(y_{test}|x_{test}, \tilde{w}_t))$ .

To approximate Bayesian inference from RUnet, Dropout is used on each convolution layer (resulting architecture is named DRUnet). As an effect of using Dropout, weights of the model and its output change for every iteration. As a result, the model of the output at a particular iteration is termed as a stochastic output. For a test input  $x_{test}$ ,  $\text{var}(y_{test})$  is the model uncertainty. As defined above, the output ROI segmentation and model uncertainty are the mean and variance of  $\tau$  stochastic outputs.

## 5. Proposed Method

To estimate model uncertainty from baseline Recurrent Unet (RUnet) architecture, the network architecture is modified by adding a dropout layer with probability 0.5 corresponding to each convolutional layer. The resulting architecture is called **DRUnet** (Recurrent Unet with Dropout). The proposed DRUnet is a supervised model which is trained to minimize the cross-entropy loss between the ground-truth ROI mask and the output of the proposed DRUnet, which is defined as:

$$\min_w \left[ -\frac{1}{n} \sum_{x=1}^n \frac{1}{\tau} \sum_{t=1}^{\tau} g(x) \log(DRU^t(x)) \right]$$

Database	Sensing Tech.	Sensor Name	Size
2000 DB1	Optical	S.D. Scanner	300×300
2000 DB2	Capacitive	TouchChip	256×364
2000 DB3	Optical	DF-90	448×478
2000 DB4	NA	Synthetic Generator	240×320
2002 DB1	Optical	TouchView II	388×374
2002 DB2	Optical	FX2000	296×560
2002 DB3	Capacitive	100 SC	300×300
2002 DB4	NA	Synthetic Generator	288×384
2004 DB1	Optical	V300	640×480
2004 DB2	Optical	U.are.U 4000	328×364
2004 DB3	Thermal	FingerChip	300×480
2004 DB4	NA	Synthetic Generator	288×384

Table 1. Description of FVC databases used in this research.

where  $n$  represents the total number of image pixels in the training images.  $g(x)$  represents the ground-truth probability of a given pixel  $x$  being a foreground pixel while  $DRU^t(x)$  represents the probability predicted by the proposed model at iteration  $t$ .  $\tau$  denotes the total number of iterations.  $w$  represents the weights of the proposed network DRU which will be fine-tuned for fingerprint ROI segmentation during training of the network.

During testing, for a given test image,  $\tau$  stochastic outputs are obtained from DRUnet. The output ROI mask is obtained as the average of stochastic outputs. While uncertainty is the variance of stochastic outputs.  $\tau=15$  is used in this study.

## 6. Databases

All the experiments in this research are conducted on publicly available Fingerprint Verification Competition (FVC) databases. Training is performed on set B consisting of total 960 images while testing is conducted on set A comprising of total 9600 fingerprint images. The ground truth segmentation is taken from [27]<sup>1</sup>. Details on FVC databases are given in Table 1.

## 7. Evaluation Metrics

### 7.1. Dice Coefficient

Dice coefficient/score [5] is a standard metric to quantify segmentation performance by comparing the overlapping region (between model’s output and the ground truth ROI mask) with the total segmented region. In terms of

<sup>1</sup>[https://figshare.com/articles/dataset/Benchmark\\_for\\_Fingerprint\\_Segmentation\\_Performance\\_Evaluation/1294209](https://figshare.com/articles/dataset/Benchmark_for_Fingerprint_Segmentation_Performance_Evaluation/1294209)

True Positive (TP), False Positive (FP) and False Negative (FN), the Dice coefficient is described as:

$$Dice = \frac{2 \times TP}{(TP + FP) + (TP + FN)}$$

## 7.2. Jaccard Similarity

We also evaluate the segmentation performance on Jaccard similarity [2], also known as Intersection over union (IoU). Jaccard similarity is defined as:

$$Jaccard = \frac{TP}{(TP + FP + FN)}$$

Though, the proposed DRU-net is an end-to-end model unlike [23, 25] which output patch wise results (which are then merged to obtain the ROI mask). For the sake of comparison, we evaluate the performance of proposed DRU-net on patch based evaluation metrics (described in Section 7.3, 7.4 and 7.5) on impression 3 and 4 of FVC 2002-Db1a database, as proposed in [23, 25].

## 7.3. Erroneously Classified Patch Percentage (Err)

Let  $p_1$  denotes a  $16 \times 16$  patch output by the segmentation algorithm and  $p_2$  denotes the corresponding ground truth patch annotated by human expert. The percentage of erroneously classified matches is defined as:

$$Err = \frac{\text{number of patches}(p_1 \neq p_2)}{\text{number of patches}(p_1)}$$

## 7.4. Hit Coefficient (HC)

Hit coefficient indicates the relative foreground fingerprint area correctly detected by the segmentation algorithm compared to the ground truth.

$$HC = \frac{\text{Area}(O \cap M)}{\text{Area}(M)}$$

where  $O$  and  $M$  denote the foreground fingerprint region detected by the segmentation algorithm and manually marked foreground respectively.

## 7.5. Mistake Coefficient (MC)

Likewise, mistake coefficient indicates the relative fingerprint area incorrectly detected as foreground by the segmentation algorithm compared to the ground truth.

$$MC = \frac{\text{Area}(O - M)}{\text{Area}(M)}$$

# 8. Results and Analysis

## 8.1. Benchmarking Results

Table 2 and Table 3 report the benchmarking results. Among the compared state-of-the-art architectures, CGan

Database	CGan	Unet	CC-Net	RUnet
2000DB1	90.58	91.28	73.98	<b>93.34</b>
2000DB2	91.10	88.53	79.66	<b>92.39</b>
2000DB3	96.23	96.74	92.52	<b>96.50</b>
2000DB4	95.11	95.44	83.03	<b>97.04</b>
2002DB1	98.15	<b>98.50</b>	93.58	98.44
2002DB2	95.18	95.84	90.88	<b>97.28</b>
2002DB3	95.91	96.61	87.70	<b>95.53</b>
2002DB4	93.69	94.02	90.08	<b>95.32</b>
2004DB1	99.18	99.24	97.33	<b>99.38</b>
2004DB2	97.58	96.60	92.34	<b>96.69</b>
2004DB3	96.93	96.34	87.96	<b>97.17</b>
2004DB4	97.14	96.95	91.65	<b>97.21</b>

Table 2. Dice score obtained on publicly available FVC Databases by various state-of-the-art segmentation algorithms.

Database	CGan	Unet	CC-Net	RUnet
2000DB1	83.56	84.79	62.08	<b>88.15</b>
2000DB2	84.27	80.72	68.05	<b>86.40</b>
2000DB3	92.96	93.78	87.06	<b>93.74</b>
2000DB4	90.75	91.33	72.86	<b>94.28</b>
2002DB1	96.39	<b>97.07</b>	88.37	96.95
2002DB2	91.35	92.32	84.02	<b>94.88</b>
2002DB3	92.38	93.56	80.05	<b>91.83</b>
2002DB4	88.23	88.78	82.58	<b>91.17</b>
2004DB1	98.38	98.50	94.91	<b>98.78</b>
2004DB2	95.37	93.50	86.12	<b>93.94</b>
2004DB3	94.12	93.03	80.29	<b>94.62</b>
2004DB4	94.53	94.15	84.92	<b>94.73</b>

Table 3. Jaccard similarity score obtained on publicly available FVC Databases by various state-of-the-art segmentation algorithms.

and CC-Net employ large backbone architectures due to which these have very high number of parameters as compared to Unet and RUnet. As a result, in fingerprint ROI segmentation task, with as limited as 960 images in the training set, these architectures do not perform as good as lighter architectures namely Unet and RUnet.

Although the performance of Unet and RUnet are competitive, however, RUnet turns out to be the best most effective baseline model for fingerprint ROI segmentation as it has been designed to improve the performance of Unet without adding a lot of parameters and thus is best suited for learning to segment fingerprint ROI (as the training dataset is fairly small).

## 8.2. Monte Carlo Dropout As An Attention Mechanism

We observe that introducing Monte Carlo Dropout along with providing model explainability (by quantifying uncertainty in prediction) helps the model to focus on impor-

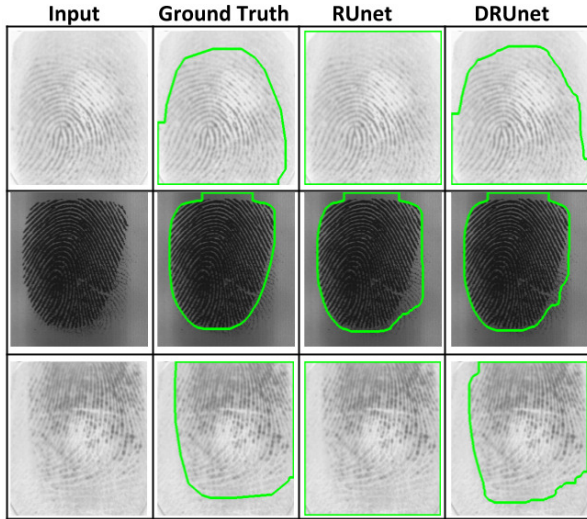


Figure 2. Sample test cases comparing the segmentation ability of RUnet before and after introduction of Monte Carlo Dropout inference mechanism (DRUnet).

Database	Jaccard Similarity		Dice Score	
	RUnet	DRUnet	RUnet	DRUnet
2000DB1	<b>88.15</b>	87.97	<b>93.34</b>	93.14
2000DB2	86.40	<b>88.43</b>	92.39	<b>93.58</b>
2000DB3	93.74	<b>95.39</b>	96.50	<b>97.57</b>
2000DB4	94.28	<b>94.89</b>	97.04	<b>97.36</b>
2002DB1	<b>96.95</b>	96.83	<b>98.44</b>	98.38
2002DB2	94.88	<b>95.13</b>	97.28	<b>97.40</b>
2002DB3	91.83	<b>93.87</b>	95.53	<b>96.73</b>
2002DB4	91.17	<b>91.53</b>	95.32	<b>95.54</b>
2004DB1	98.78	<b>98.98</b>	99.38	<b>99.49</b>
2004DB2	93.94	<b>95.98</b>	96.69	<b>97.93</b>
2004DB3	94.62	<b>95.29</b>	97.17	<b>97.55</b>
2004DB4	94.73	<b>96.18</b>	97.21	<b>98.03</b>

Table 4. Comparison of Jaccard similarity and Dice Score obtained by RUnet and proposed DRUnet.

tant features. As a result, as reported in Table 4 overfitting is reduced and improved segmentation performance is achieved using proposed DRUnet compared to baseline RUnet. Figure 2 presents qualitative comparison of RUnet and DRUnet. RUnet misclassifies background pixels as foreground when the background pixels have similar intensity as the foreground pixels. DRUnet on the other hand has marginalized weights as a result of introducing Monte Carlo Dropout inference mechanism. Due to this, Monte Carlo Dropout acts like an attention mechanism and helps DRUnet to learn more robust features and obtain superior performance as compared to RUnet.

### 8.3. Uncertainty Predicted by DRUnet

While designing an explainable fingerprint ROI segmentation algorithm which can output uncertainty in model’s prediction, it is expected that the model should exhibit higher uncertainty around unclear ridge structure and noisy background. Furthermore, the model should output higher uncertainty in case of incorrect segmented pixels. As shown in first and second column (from left) of Figure 3, background pixels with similar intensity are incorrectly predicted as foreground by proposed DRUnet. However, interestingly the model uncertainty predicted for these pixels is fairly high which gives an indication that the model is not confident in its prediction and some erroneous predictions could have been made by DRUnet. Likewise in third, fourth and fifth column, the ROI is correctly segmented and the model outputs very low uncertainty values. Uncertainty value in third column is higher compared to fourth and fifth column since the background in input image corresponding to third column has more noise and similar intensity values as the foreground due to which it is more difficult for DRUnet to segment it compared to the other two images.

### 8.4. Successful Cases of Segmentation

Sample successful cases of fingerprint ROI segmentation are presented in Figure 4. We observe that the proposed DRUnet works well across all the datasets used for experimental evaluation. As can be seen in Figure 4, DRUnet can differentiate background and foreground ridge details in fingerprint images acquired through different sensors. Thus, we observe that DRUnet exhibits good generalization ability across a variety of background and sensor noise originating from different fingerprint sensors.

### 8.5. Failure Cases of Segmentation

Although effectiveness of DRUnet is observed across various experiments, however, as shown in Figure 5 we do find cases when DRUnet obtains unsatisfactory performance. We observe that DRUnet misclassifies the background noise as foreground fingerprint region when the intensity of background pixels is similar to the foreground pixels.

### 8.6. Comparison with State-of-the-art

Dice score and Jaccard similarity score obtained by the proposed DRUnet are compared with the recently proposed fingerprint ROI segmentation algorithm [23] in Table 5. We observe that DRUnet outperforms [23] on some datasets while achieves competitive performance on other datasets. Results on other evaluation metrics are reported in Table 6. We argue that better segmentation performance of [23] compared to DRUnet is due to the availability of small amount of training dataset for DRUnet. [23] is trained

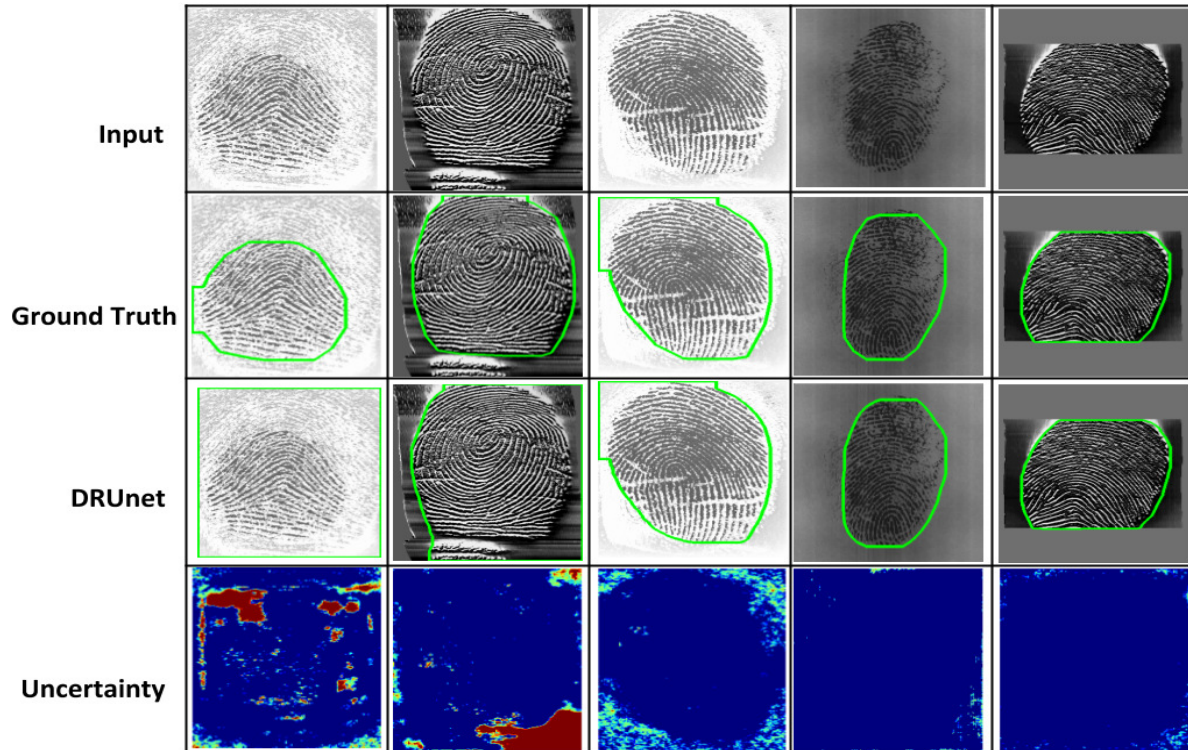


Figure 3. Sample cases of uncertainty predicted by DRUnet. Blue and red color denote low and high uncertainty values respectively.

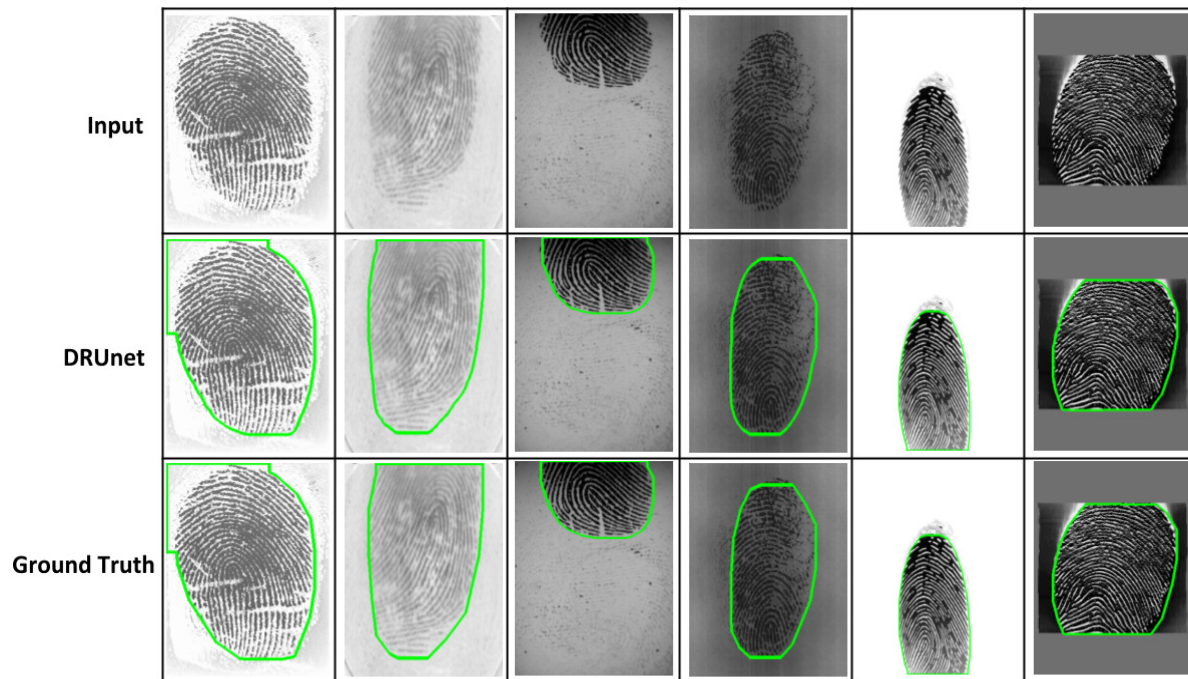


Figure 4. Sample successful cases of ROI segmentation by proposed DRUnet.

on patches of size  $16 \times 16$  to classify the fingerprint patch as foreground or background. Thus, the number of training patches are large enough to train the model. However, since [23] outputs a label on patch level, it requires post-

processing to obtain the output ROI mask. DRUnet on the other hand, is an end-to-end model trained on full sized images due to which the size of training dataset is very small to train it. However, competitive segmentation performance

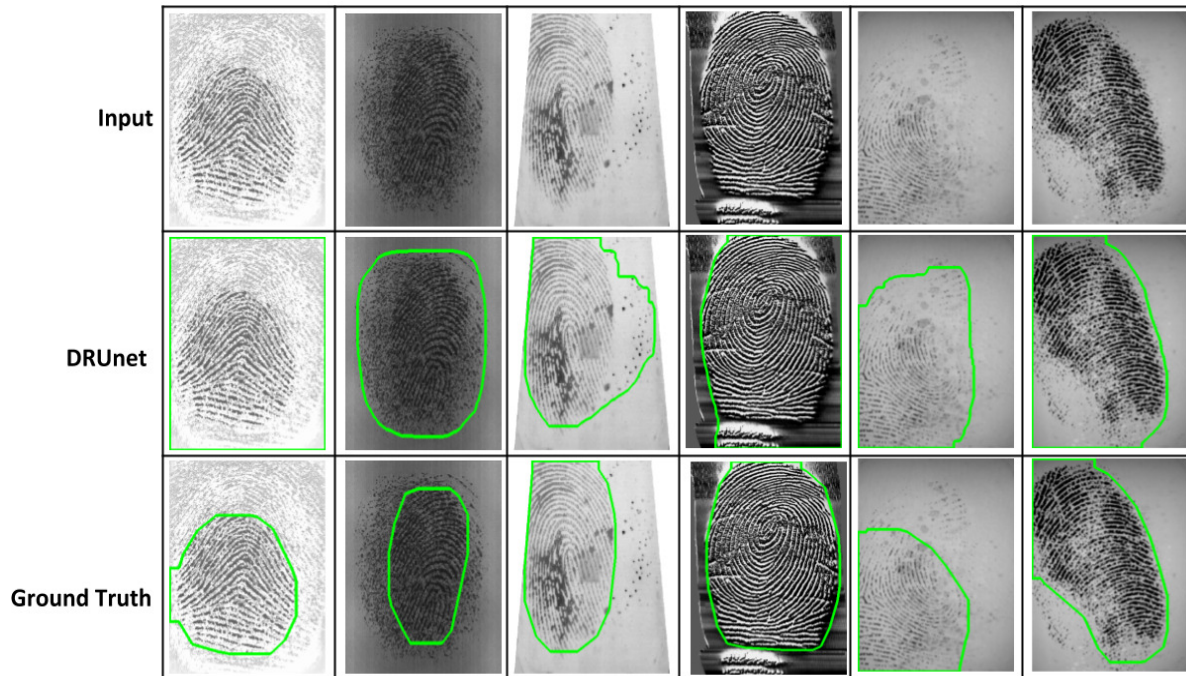


Figure 5. Sample failure cases of ROI segmentation by proposed DRUnet.

Database	Jaccard Similarity		Dice Score	
	DRUnet	[23]	DRUnet	[23]
2000DB1	87.97	<b>95.86</b>	93.14	<b>97.36</b>
2000DB2	88.43	<b>95.69</b>	93.58	<b>97.20</b>
2000DB3	95.39	<b>96.98</b>	<b>97.57</b>	97.40
2000DB4	94.89	<b>97.42</b>	97.36	<b>97.99</b>
2002DB1	96.83	<b>98.22</b>	<b>98.38</b>	98.18
2002DB2	95.13	<b>96.64</b>	<b>97.40</b>	97.37
2002DB3	93.87	<b>96.10</b>	<b>96.73</b>	96.26
2002DB4	91.53	<b>94.91</b>	95.54	<b>95.75</b>
2004DB1	<b>98.98</b>	98.89	<b>99.49</b>	97.88
2004DB2	95.98	<b>96.60</b>	<b>97.93</b>	96.97
2004DB3	95.29	<b>97.39</b>	97.55	<b>97.97</b>
2004DB4	96.18	<b>96.59</b>	<b>98.03</b>	97.20

Table 5. Comparison of Jaccard similarity and Dice Score obtained on publicly available FVC Databases with state-of-the-art fingerprint segmentation algorithm.

achieved by DRUnet as compared to [23] demonstrates the effectiveness of proposed work.

Algorithm	Err	HC	MC
[23]	<b>0.0159</b>	0.9845	<b>0.0146</b>
[25]	0.0365	0.9421	0.0747
<b>DRUnet (Proposed)</b>	<i>0.0173</i>	<b>0.9949</b>	<i>0.0313</i>

Table 6. Comparison of average error, hit coefficient and mistake coefficient by proposed DRUnet with state-of-the-art segmentation algorithms.

## 9. Conclusion and Future Work

This paper is the first work to propose an explainable fingerprint ROI segmentation algorithm. Firstly, benchmarking of four state-of-the-art segmentation algorithm is performed on fingerprint ROI segmentation task. Later, model uncertainty is introduced on the best performing model. Experimental results and visualizations demonstrate the fact that introducing Monte Carlo Dropout works like an attention mechanism and also provides model’s confidence in prediction. We show that proposed model correctly outputs model confidence by predicting higher uncertainty around highly noisy and incorrectly predicted fingerprint regions, and low uncertainty value around regions with clear ridge structure and low background noise. In future, other methods on uncertainty quantification can be explored.

## 10. Acknowledgement

Authors thank the HPC facility of Inria Sophia Antipolis for computational resources used in this research. This work is partly supported by the French Government (National Research Agency, ANR) under grant agreement ANR-18-CE92-0024. I. Joshi is partially supported by the Raman Charpak Fellowship 2019.

## References

- [1] Charles Blundell, Julien Cornebise, Koray Kavukcuoglu, and Daan Wierstra. Weight uncertainty in neural networks. In *Proceedings of the 32nd International Conference on In-*

- ternational Conference on Machine Learning-Volume 37, pages 1613–1622, 2015.
- [2] Seung-Seok Choi, Sung-Hyuk Cha, and Charles C Tappert. A survey of binary similarity and distance measures. *Journal of Systemics, Cybernetics and Informatics*, 8(1):43–48, 2010.
  - [3] Marc Combalia, Ferran Hueto, Susana Puig, Josep Malvehy, and Veronica Vilaplana. Uncertainty estimation in deep neural networks for dermoscopic image classification. In *Proceedings of the IEEE/CVF Conference on Computer Vision and Pattern Recognition Workshops*, pages 744–745, 2020.
  - [4] Raimundo Claudio da Silva Vasconcelos and Hélio Pedrini. Fingerprint image segmentation based on oriented pattern analysis. In *VISIGRAPP (4: VISAPP)*, pages 405–412, 2019.
  - [5] Lee R Dice. Measures of the amount of ecologic association between species. *Ecology*, 26(3):297–302, 1945.
  - [6] Mamdouh F Fahmy and MA Thabet. A fingerprint segmentation technique based on morphological processing. In *IEEE International Symposium on Signal Processing and Information Technology*, pages 000215–000220, 2013.
  - [7] Pedro M Ferreira, Ana F Sequeira, and Ana Rebelo. A fuzzy c-means algorithm for fingerprint segmentation. In *Iberian Conference on Pattern Recognition and Image Analysis*, pages 245–252, 2015.
  - [8] Yarin Gal and Zoubin Ghahramani. Bayesian convolutional neural networks with bernoulli approximate variational inference. *arXiv preprint arXiv:1506.02158*, 2015.
  - [9] Yarin Gal and Zoubin Ghahramani. Dropout as a bayesian approximation: Representing model uncertainty in deep learning. In *international conference on machine learning*, pages 1050–1059, 2016.
  - [10] Chunfeng Hu, Jianping Yin, En Zhu, Hui Chen, and Yong Li. A composite fingerprint segmentation based on log-gabor filter and orientation reliability. In *2010 IEEE International Conference on Image Processing*, pages 3097–3100, 2010.
  - [11] Zilong Huang, Xinggang Wang, Lichao Huang, Chang Huang, Yunchao Wei, and Wenyu Liu. Ccnet: Criss-cross attention for semantic segmentation. In *Proceedings of the IEEE International Conference on Computer Vision*, pages 603–612, 2019.
  - [12] P. Isola, J. Zhu, T. Zhou, and A. A. Efros. Image-to-image translation with conditional adversarial networks. In *IEEE Conference on Computer Vision and Pattern Recognition*, 2017.
  - [13] I. Joshi, A. Anand, M. Vatsa, R. Singh, S. Dutta Roy, and P. K. Kalra. Latent fingerprint enhancement using generative adversarial networks. In *2019 IEEE Winter Conference on Applications of Computer Vision (WACV)*, pages 895–903, 2019.
  - [14] Alex Kendall, Vijay Badrinarayanan, and Roberto Cipolla. Bayesian segnet: Model uncertainty in deep convolutional encoder-decoder architectures for scene understanding. *arXiv preprint arXiv:1511.02680*, 2015.
  - [15] Alex Kendall and Yarin Gal. What uncertainties do we need in bayesian deep learning for computer vision? In *Advances in neural information processing systems*, pages 5574–5584, 2017.
  - [16] Alex Kendall, Yarin Gal, and Roberto Cipolla. Multi-task learning using uncertainty to weigh losses for scene geometry and semantics. In *Proceedings of the IEEE conference on computer vision and pattern recognition*, pages 7482–7491, 2018.
  - [17] Yongchan Kwon, Joong-Ho Won, Beom Joon Kim, and Myunghee Cho Paik. Uncertainty quantification using bayesian neural networks in classification: Application to biomedical image segmentation. *Computational Statistics & Data Analysis*, 142:106816, 2020.
  - [18] Balaji Lakshminarayanan, Alexander Pritzel, and Charles Blundell. Simple and scalable predictive uncertainty estimation using deep ensembles. In *Advances in neural information processing systems*, pages 6402–6413, 2017.
  - [19] Eryun Liu, Heng Zhao, Fangfei Guo, Jimin Liang, and Jie Tian. Fingerprint segmentation based on an adaboost classifier. *Frontiers of Computer Science in China*, 5(2):148–157, 2011.
  - [20] Christos Louizos and Max Welling. Multiplicative normalizing flows for variational bayesian neural networks. In *Proceedings of the 34th International Conference on Machine Learning-Volume 70*, pages 2218–2227, 2017.
  - [21] Andrey Malinin and Mark Gales. Predictive uncertainty estimation via prior networks. In *Advances in Neural Information Processing Systems*, pages 7047–7058, 2018.
  - [22] Olaf Ronneberger, Philipp Fischer, and Thomas Brox. U-Net: Convolutional Networks for Biomedical Image Segmentation. pages 234 – 241, 2015.
  - [23] Paulo Bruno S Serafim, Aldísio G Medeiros, Paulo AL Rego, José Gilvan R Maia, Fernando AM Trinta, Marcio EF Maia, José Antonio F Macêdo, and Aloísio V Lira Neto. A method based on convolutional neural networks for fingerprint segmentation. In *2019 International Joint Conference on Neural Networks (IJCNN)*, pages 1–8, 2019.
  - [24] Nitish Srivastava, Geoffrey Hinton, Alex Krizhevsky, Ilya Sutskever, and Ruslan Salakhutdinov. Dropout: a simple way to prevent neural networks from overfitting. *The journal of machine learning research*, 15(1):1929–1958, 2014.
  - [25] Branka Stojanović, Oge Marques, Aleksandar Nešković, and Snežana Puzović. Fingerprint roi segmentation based on deep learning. In *2016 24th Telecommunications Forum (TELFOR)*, pages 1–4, 2016.
  - [26] Raoni FS Teixeira and Neucimar J Leite. Unsupervised fingerprint segmentation based on multiscale directional information. In *Iberoamerican Congress on Pattern Recognition*, pages 38–46, 2011.
  - [27] Duy Hoang Thai and Carsten Gottschlich. Global variational method for fingerprint segmentation by three-part decomposition. *IET Biometrics*, 5(2):120–130, 2016.
  - [28] Duy Hoang Thai, Stephan Huckemann, and Carsten Gottschlich. Filter design and performance evaluation for fingerprint image segmentation. *PLoS one*, 11(5):e0154160, 2016.
  - [29] Aleksei Ustimenko, Liudmila Prokhorenkova, and Andrey Malinin. Uncertainty in gradient boosting via ensembles. *arXiv preprint arXiv:2006.10562*, 2020.
  - [30] Wei Wang, Kaicheng Yu, Joachim Hugonot, Pascal Fua, and Mathieu Salzmann. Recurrent u-net for resource-constrained

segmentation. In *Proceedings of the IEEE International Conference on Computer Vision*, pages 2142–2151, 2019.

- [31] Gongping Yang, Guang-Tong Zhou, Yilong Yin, and Xiukun Yang. K-means based fingerprint segmentation with sensor interoperability. *EURASIP Journal on Advances in Signal Processing*, 2010(1):729378, 2010.